

The Thickness of Stellar Disks in Early-type Galaxies

E. M. Chudakova* and O. K. Sil’chenko**

Sternberg Astronomical Institute, Lomonosov Moscow State University, Moscow, Russia

Received August 19, 2013; in final form, October 30, 2013

Abstract—We suggest and justify a new photometric method enabling the derivation of the relative thickness of a galactic disk from the two-dimensional surface-brightness distribution of the galaxy in the plane of the sky. The method is applied to images of 45 early-type (S0–Sb) galaxies with known radial exponential or piece-wise-exponential (with a flatter outer profile) surface-brightness distributions. The data were taken from the open SDSS archive. The statistics of the estimated relative thicknesses of the stellar disks of early-type galaxies show the following features. The disks of lenticular and spiral early-type galaxies have similar thickness. The presence of a bar results in only a slight increase of the thickness. However, there is a substantial difference between the thicknesses of disks with a single exponential brightness profile and exponential disks that represent the inner segments of Type III profiles (after Erwin); i.e., they have an outer exponential disk with a larger characteristic scale. The disks are significantly thicker in the former than in the latter case. This may provide evidence that a single exponential scale in a disk surface-brightness distribution forms due to viscosity effects acting over the entire period of star-formation evolution in the disk.

DOI: 10.1134/S1063772914050023

1. INTRODUCTION

The two main large-scale structural components of a galaxy—the bulge and disk—have different geometries. Bulges are spheroids, with generally three comparable axes, while disks are “flat” stellar subsystems whose thicknesses are appreciably smaller than their radii. However, the thickness of the disks is not infinitely small, and the thickness and radius of a typical galactic disk differ by less than an order of magnitude, and often are comparable. The thickness of the stellar disk is an important physical parameter that can serve as a guide to the dynamical evolution of a galaxy: interactions with other galaxies such as gravitational tides or mergers with smaller satellites can “heat” the disks [1, 2], making them thicker, while the smooth, laminar accretion of a large amount of cool gas with subsequent star formation and the development of young stellar systems that are cool like the gas from which they form can reduce the thickness of the disk [3].

Observational studies of the thicknesses of stellar disks in galaxies have been based mainly on statistics using large, mixed samples of galaxies. It has also been assumed that the disks are randomly oriented in space, so that the distribution of apparent eccentricities for the disks projected onto the plane of the sky carries information about the average ratio

of the thickness to the radius. The latest statistical estimates of the average thicknesses of galactic disks q are based on the data from SDSS: Padilla and Strauss [4] analyzed a sample of several thousand galaxies with exponential outer brightness profiles—i.e., galaxies with disks—from the sixth release of the SDSS, obtaining $q = 0.21 \pm 0.02$. The same team obtained the somewhat higher estimate $q = 0.267 \pm 0.009$ using naked eye classifications of spiral galaxies from the Galaxy Zoo project, selected from the eighth release of the SDSS [5].

There are not very many individual, non-statistical estimates of the thicknesses of stellar disks. It is possible to measure the thickness of a stellar disk directly only if the galaxy is viewed edge-on. Note that it is difficult to estimate other properties of the disk structure in this case, since all the material that is located in the equatorial plane is integrated along the line of sight. In early studies of the surface-brightness distributions in the optical (*BVRI*) in eight S0–Sd galaxies viewed edge-on [6], very thin disks were found—the ratio of the vertical and horizontal scale heights for the brightness distributions were, on average, $z_0/h = 0.17 \pm 0.01$. However, this may have been due to the small size of the sample: recently, based on a decomposition of the near-IR images of some two hundred edge-on galaxies (*JHK*-band images from the 2MASS survey), Mosenkov et al. [7] found a very broad distribution of z_0/h with a median close to 0.3.

*E-mail: artenik@gmail.com

**E-mail: olga@sai.msu.ru

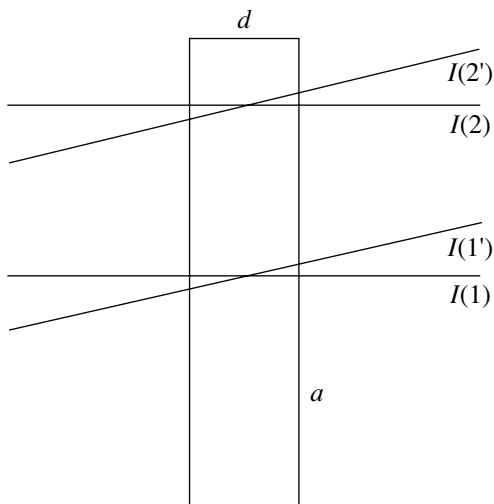


Fig. 1. Schematic showing the integration of the disk surface brightness along the line of sight for various disk inclinations to the plane of the sky. The disk is depicted edge-on, and the observer's line of sight is in the plane of the sky.

Meanwhile, the average thickness of galactic disks has no more value than the mean temperature in a hospital. Galactic disks can display very different dynamic evolution, due primarily to the density of the environment, as well as the prominence and structure of the spheroidal components of the galaxy. Accordingly, the distribution of disk thickness is far from a normal law. The measurement of individual disk thicknesses and comparison with the statistics of other disk parameters, such as the surface-brightness profiles, is a more interesting problem. This is the question addressed in the present study.

We propose here a new method, which we have used to estimate individual disk thicknesses in a sample of galaxies viewed at angles different from 90° . We were interested in possible differences in disk thicknesses in galaxies with different radial surface-brightness profiles. We used the sample of galaxies and classification of the radial brightness profiles compiled in [8, 9]. In contrast to the classical study of Freeman [10], which reported strictly exponential surface-brightness distributions in the stellar galactic disks, Erwin et al. [8] and Guti'erez et al. [9] found that, in general, a disk surface-brightness profile can be represented by two exponential sections with different characteristic scales. It is currently believed that single-exponential disks with a uniform scale (Type I), truncated disks (outer scale smaller than inner scale, Type II), and two-tiered disks (outer scale larger than inner scale, Type III) have different origins. Previously proposed scenarios have predicted definite consequences for the disk thicknesses. Thus,

our results can be used to test theories of the formation and evolution of galactic disks.

2. METHOD

We have developed an original method that can be used to estimate relative disk thicknesses using the two-dimensional surface-brightness distribution of the disk projected onto the plane of the sky. The method is applicable for galaxies with circular disks with exponential or piecewise-exponential surface-brightness profiles. The disks are considered to be plane-parallel (within one exponential section of the brightness profile), i.e., to have the same thickness at any distance from the center. We assumed that the same exponential law for the decline of the volumetric brightness is obeyed in the equatorial plane and at some distance from this plane. In addition, for the method to work correctly, it is necessary that the galaxy not be viewed strictly face-on or strictly edge-on. The key idea of our approach is splitting the galaxy image into sectors. The lines of equal surface brightness (isophotes) and measurements of the exponential scale for different angles to the major axis of the isophotes provide discrete sets of points separated by equal angles in polar coordinates referenced to the center of the galaxy and its line of nodes. Both the isophotes and measurements of the exponential scale were fitted by ellipses. This approach makes it possible to estimate separately the oblateness of the isophotes and of the ellipses for the scale coefficients; we find the relative disk thickness by comparing these two ellipticities.

2.1. Main Formulas

Let us consider a galaxy with a circular disk with radius a , relative thickness $q = d/a$ and inclination to the plane of the sky i . The ellipticity of the isophotes e_I of such a galaxy is related to the thickness and inclination by the formula

$$\sin i = \sqrt{\frac{2e_I - e_I^2}{1 - q^2}}. \quad (1)$$

Let us assume that the disk surface brightness has an exponential dependence on the radius, expressed in the plane of the galaxy by the formula $I(R) = I(0) \exp(-R/h)$ [10]. Let us compare the brightnesses of points 1 and 2 (Fig. 1) for observations along the rotation axis of the disk ($I(1)$ and $I(2)$) and at some angle to the axis ($I(1')$ and $I(2')$). We assume that the disk thickness d is constant and the radial scale h does not depend on the distance to the galactic plane. The surface brightness at a given point of the disk is the integral of the volumetric

brightness along the line of sight. For the lines of sight corresponding to $I(1)$ and $I(2)$, the volumetric brightness at each point of parallel segments of the lines of sight over which we integrate have the same ratio, $I(1)/I(2) = \exp(\rho_{12}/h)$. If d is taken to be constant in the radial direction and h to be constant with height, the proportionality is retained at each point of the lines of sight corresponding to $I(1')$ and $I(2')$. Therefore, $I(1')/I(2') = \exp(\rho_{12}/h)$. Thus, the scale h observed along a line of nodes does not depend on the inclination of the line of sight to the galactic plane. Simultaneously, the scale h measured in the plane of the sky *at an angle* to the line of nodes will decrease, solely due to the effect of projection, showing a cosine dependence on the polar angle. Thus, having constructed an ellipse for the distribution of the apparent scale in azimuth in the plane of the sky and measured the ellipticity of this figure e_h , we can find the inclination of the galactic disk to the plane of the sky i from the relation

$$\sin i = \sqrt{2e_h - e_h^2}. \quad (2)$$

Thus, inserting (2) into (1), we obtain the following expression for the thickness of a galactic disk in terms of the ellipticities of an isophote and of the azimuthal distribution of the scale:

$$q = \sqrt{1 - \frac{2e_I - e_I^2}{2e_h - e_h^2}}. \quad (3)$$

2.2. Computation Stages

Prior to the computations, the background was subtracted from the galaxy image, and stars and bright, compact features such as rings and star-formation regions were masked.

An approximate isophote $R_n(\text{count})$ can be determined from the equation $I_n(R_n) = \text{count}$ for a given number of counts *count*. An ellipse with semi-major axis a_I and ellipticity e_I fitted to a set of 20 points uniformly distributed in azimuth in polar coordinates, $M_n(\text{count}) = \left(R_n, \frac{\pi n}{10} + \frac{\pi}{20}\right)$, approximates the galaxy isophote at the brightness level *count*.

We divided the cleaned galaxy image into sectors. We took the center to correspond to the brightest point, and divided the image into 20 non-intersecting sectors with opening angle $\pi/10$. We constructed the surface-brightness distribution $I'_n(\rho)$ for the n th sector—the dependence of the mean brightness I' on the distance ρ from the center for the azimuthal angles $\varphi \in \left(\frac{\pi n}{10}; \frac{\pi(n+1)}{10}\right]$. If the galaxy has mirror symmetry, the profiles $I'_n(\rho)$ and

$I'_{n+10}(\rho)$ are similar, and it is reasonable to increase the accuracy of measurements by considering 10 profiles, $I_n(\rho) = (I'_n(\rho) + I'_{n+10}(\rho))/2$. Assuming an exponential radial dependence for the disk surface brightness, we calculated the scale h_n for each of the 10 sector cross sections. For this purpose, we fitted the least-squares line $1.086(R_m/h) + l$ to the set of points $(R_m, 2.5 \log I_n(R_m))$, where $R_m \in [R_{n0}(j), R_n(\text{count})]$. We found the R_{n0} with the smallest least-squares error for each cross-section. Then, $h_n = h(R_{n0})$ is the scale for the n th cross section in the section $[R_{n0}(\text{count}), R_n(\text{count})]$. The set of points in polar coordinates $N_n = \left(h_n, \frac{\pi n}{10} + \frac{\pi}{20}\right)$ is approximated by the ellipse corresponding to the scales, with semi-major axis a_h and ellipticity e_h .

For each Type III galaxy, for which the full inner surface-brightness profile is approximated by two exponential pieces, we constructed the isophote and ellipse of the scale coefficients for each of the two exponential segments separately. The thickness of the disk was derived using (3).

3. GALAXY SAMPLE AND DATA

To test the method, we compiled a sample of galaxies with exponential and piecewise-exponential disks, described in [8, 9]. Galaxies with bars are described in [8], and galaxies without bars in [9]. We selected galaxies with single-exponential disks (Type I) and with piecewise-exponential disks, with the scale of the outer disk larger than the scale for the inner disk (Type III), from the total sample presented in [8, 9]. Our resulting sample includes 66 galaxies: 29 Type I and 37 Type III. The sample contains mainly early-type (S0–Sb) objects. We searched for digital images of the sample galaxies in the photometric survey of the SDSS [11]. Images were found for 24 Type I and 19 Type III galaxies. We adopted archival SCORPIO data from the 6-m telescope of the Special Astrophysical Observatory for NGC 2300 and NGC 2787 [12]. We applied our method to the SDSS r images, which have the highest signal-to-noise ratio. It proved impossible to apply the method to NGC 2712 (Type I; the disk was non-exponential), NGC 4045 (Type III; the inner disk was non-exponential, and the outer disk noisy), NGC 5806 (Type III; the inner disk displays a high intrinsic eccentricity), UGC 4599 (Type III; the noise level hindered separate of the low-surface-brightness disk). We also added the galaxies NGC 4513 (Type III [13]) and NGC 4124 (Type I [14]) to the sample.

As a result, we successfully applied our method to find the relative disk thicknesses for 26 Type I galaxies, 17 inner disks of Type III galaxies, and 2 outer disks of Type III galaxies.

Relative stellar-disk thicknesses found using our new photometric method

| Galaxy | Type | R_{25} | Disk type after [8, 9] | h | R_0 | R_I | q | δq |
|----------|--------------------------|----------|---------------------------|------|-------|-------|--------|------------|
| 1 | 2 | 3 | 4 | 5 | 6 | 7 | 8 | 9 |
| IC 676 | (R)SB(r)0+ | 40'' | I | 72'' | — | 61'' | 0.3790 | 0.0001 |
| NGC 1022 | (R')SB(s)a | 61 | I | 56 | — | 97 | 0.808 | 0.012 |
| NGC 2787 | SB(r)0+ | 95 | I | 85 | — | 114 | 0.230 | 0.008 |
| NGC 3485 | SB(r)b | 47 | I | 92 | — | 47 | 0.70 | 0.02 |
| NGC 4151 | (R')SAB(rs)ab | 90 | I | 90 | — | 90 | 0.45 | 0.04 |
| NGC 4245 | SB(r)0/a | 65 | I | 78 | — | 88 | 0.687 | 0.006 |
| NGC 4267 | SB(s)0-? | 74 | I | 76 | — | 74 | 0.48 | 0.01 |
| NGC 4340 | SB(r)0+ | 74 | I | 149 | — | 74 | 0.524 | 0.009 |
| NGC 4477 | SB(s)0:? | 114 | I | 85 | — | 88 | 0.69 | 0.03 |
| NGC 4596 | SB(r)0+ | 182 | I | 174 | — | 102 | 0.664 | 0.014 |
| NGC 4643 | SB(rs)0/a | 105 | I | 182 | — | 104 | 0.73 | 0.02 |
| NGC 4665 | SB(s)0/a | 107 | I | 145 | — | 106 | 0.812 | 0.007 |
| NGC 4754 | SB(r)0-: | 114 | I | 129 | — | 113 | 0.34 | 0.02 |
| NGC 5750 | SB(r)0/a | 70 | I | 42 | — | 70 | 0.0 | 0.012 |
| NGC 7743 | (R)SB(s)0+ | 57 | I | 68 | — | 75 | 0.50 | 0.04 |
| NGC 2300 | SA0 ⁰ | 85 | I | 416 | — | 187 | 0.565 | 0.023 |
| NGC 3032 | SAB(r)0 ⁰ | 36 | I | 36 | — | 36 | 0.415 | 0.016 |
| NGC 3169 | SA(s)a | 125 | I | 126 | — | 125 | 0.40 | 0.05 |
| NGC 3599 | SA0 | 16 | I | 34 | — | 30 | 0.706 | 0.007 |
| NGC 3607 | SA(s)0 ⁰ | 114 | I | 103 | — | 114 | 0.31 | 0.11 |
| NGC 3626 | (R)SA(rs)0+ | 71 | I | 64 | — | 49 | 0.52 | 0.02 |
| NGC 4578 | SA(r)0 ⁰ | 72 | I | 79 | — | 72 | 0.0 | 0.02 |
| NGC 4772 | SA(s)a | 107 | I | 116 | — | 106 | 0.31 | 0.02 |
| NGC 5485 | SA0 pec | 58 | I | 55 | — | 58 | 0.43 | 0.02 |
| NGC 5520 | Sb | 37 | I | 38 | — | 36 | 0.214 | 0.014 |
| NGC 4124 | SA0 ⁺ (r) | 100 | I | 74 | — | 100 | 0.0 | 0.007 |
| NGC 3489 | SAB0 ⁺ (rs) | 87 | III | 56 | 54'' | 111 | 0.0 | 0.03 |
| NGC 4371 | SB0 ⁺ (r) | 113 | III | 154 | 126 | 149 | 0.362 | 0.008 |
| NGC 4612 | (R)SAB0 ⁰ | 68 | III (exter) | 98 | 44 | 88 | 0.516 | 0.020 |
| NGC 4612 | (R)SAB0 ⁰ | 68 | III (inter) | 38 | 10 | 40 | 0.192 | 0.006 |
| NGC 4691 | (R)SB(s)0/a pec | 71 | III | 105 | 32 | 65 | 0.715 | 0.013 |
| NGC 4699 | SAB(rs)b | 130 | III (exter) | 98 | 49 | 98 | 0.564 | 0.007 |
| NGC 4699 | SAB(rs)b | 130 | III (inter) | 34 | 18 | 42 | 0.258 | 0.013 |
| NGC 5740 | SAB(rs)b | 61 | III | 46 | 27 | 69 | 0.0 | 0.018 |
| NGC 7177 | SAB(r)b | 53 | III | 42 | 34 | 49 | 0.16 | 0.04 |
| NGC 3619 | (R)SA0 ⁻ (s): | 81 | III | 82 | 42 | 82 | 0.22 | 0.03 |
| NGC 3898 | SA(s)ab | 94 | III | 77 | 41 | 81 | 0.175 | 0.007 |
| NGC 3900 | SA0 ⁺ (r) | 67 | III | 70 | 50 | 100 | 0.195 | 0.008 |
| NGC 3998 | SA0 ⁰ (r)? | 71 | III | 57 | 57 | 113 | 0.35 | 0.03 |
| NGC 4138 | SA0 ⁺ (r) | 65 | III | 39 | 19 | 46 | 0.066 | 0.008 |
| NGC 4459 | SA0 ⁺ (r) | 32 | III | 38 | 16 | 45 | 0.524 | 0.024 |
| NGC 7457 | SA0 ⁻ (rs)? | 92 | III | 48 | 12 | 27 | 0.20 | 0.02 |
| NGC 3604 | SA(s)a pec | 41 | III | 45 | 28 | 55 | 0.15 | 0.01 |
| NGC 4150 | SA0 ⁰ (r)? | 45 | III | 30 | 32 | 68 | 0.0 | 0.004 |
| NGC 4513 | (R)SA0 ⁰ | 26 | III | 28 | 14 | 26 | 0.245 | 0.004 |

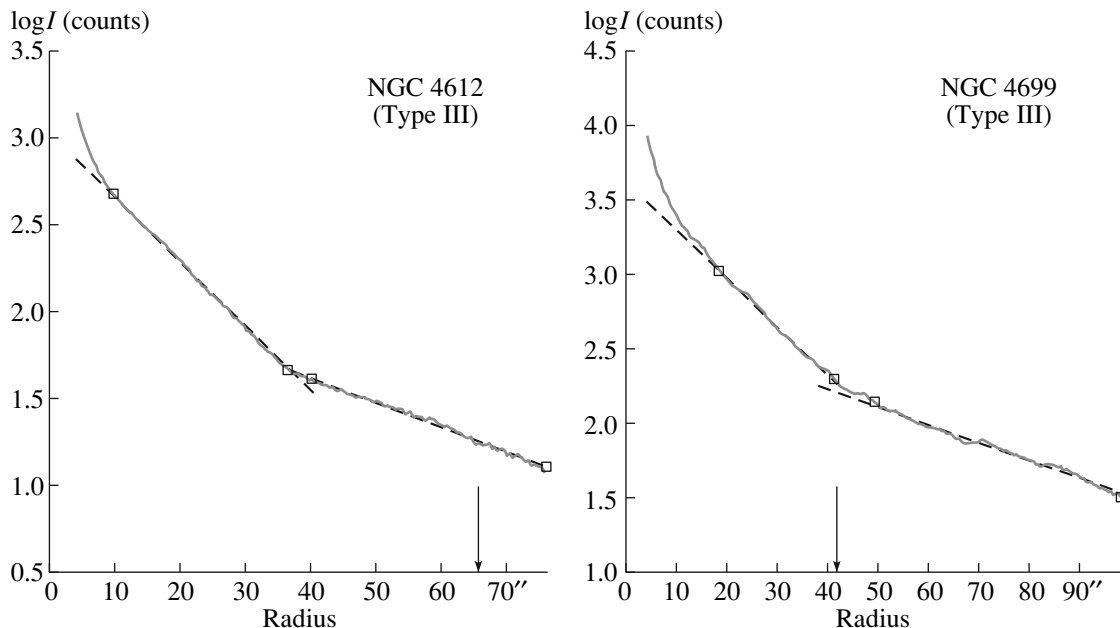


Fig. 2. Piecewise-exponential surface-brightness profiles of the Type III galaxies NGC 4612 and NGC 4699 in the SDSS r filter.

4. RESULTS

The accuracy of the SDSS data was sufficient to derive the thickness of both the inner and outer disks for only two Type III galaxies: NGC 4612 and NGC 4699. Figure 2 presents the brightness profiles in the cross sections of the major axes of the inner disks of these galaxies. The arrow marks the isophotal radius at the level $\mu_r = 23.5$, which is the surface brightness *count* at which we aimed to draw the reference isophotes. The outer disk in NGC 4612 is probably the main (Freeman) disk, while the outer disk in NGC 4699 is located beyond the formal optical boundary of the galaxy and has low surface brightness. Nevertheless, the outer-disk parameters are surprisingly close: in both cases, the outer disks are thick ($q = 0.52$ – 0.56), and much thicker than the inner disks ($q = 0.19$ – 0.26). Since we already found a similar ratio of the inner and outer disk thicknesses for the Type III galaxy NGC 7217 from kinematic data [15], this hints at some regularity, with the outer disks most often being thicker than the inner ones.

Complete results for the total sample are presented in the Table, whose columns contain (1) the galaxy name, (2) the morphological type according to the NED database, (3) the semi-major axis of the galaxy image according to the NED data, (4) the type of brightness distribution over the disk according to [8, 9], (5) the exponential scale along the line of nodes according to our results, (6) the inner boundary of the disk in Type III galaxies, (7) the radius at which the reference isophote was drawn, (8) the relative

disk thickness according to our results, and (9) the statistical uncertainty in the relative disk thickness.

The following figures present the statistics of our results for the relative thicknesses of the stellar disks, presented as histograms. The horizontal axis plots the disk thickness q and the vertical axis the number of galaxies in the subsamples in a specified thickness range. Galaxies for which the eccentricities of the isophote and scale are similar enough that the argument of the square root in (3) is formally negative due to the statistical uncertainty in q are plotted using negative q values. We take such disks to be infinitely thin, but plot them to the left of zero, in the “complex” range.

In the histogram for the complete sample (Fig. 3), the mean disk thickness is 0.38. The histogram for the entire sample is very wide, with relative thicknesses ranging from 0 to 0.9. If we break down the sample according to the type of disk, the picture changes. Figure 4 shows that the distributions of the inner-disk thickness for the Type III galaxies and of the overall disk thickness for the Type I galaxies have shifted maxima. In addition, the internal scatter of the values is smaller than for the total sample. The inner disks of the Type III galaxies have a mean thickness of 0.19, while the disks of the Type I galaxies have a mean thickness of 0.48. Despite the small sizes of the samples, a Kolmogorov–Smirnov test indicates that the probability that the disks of Type I galaxies and the inner disks of Type III galaxies belong to the same parent sample is only 0.7%; i.e., the relative disk thicknesses for Type I and Type III galaxies are

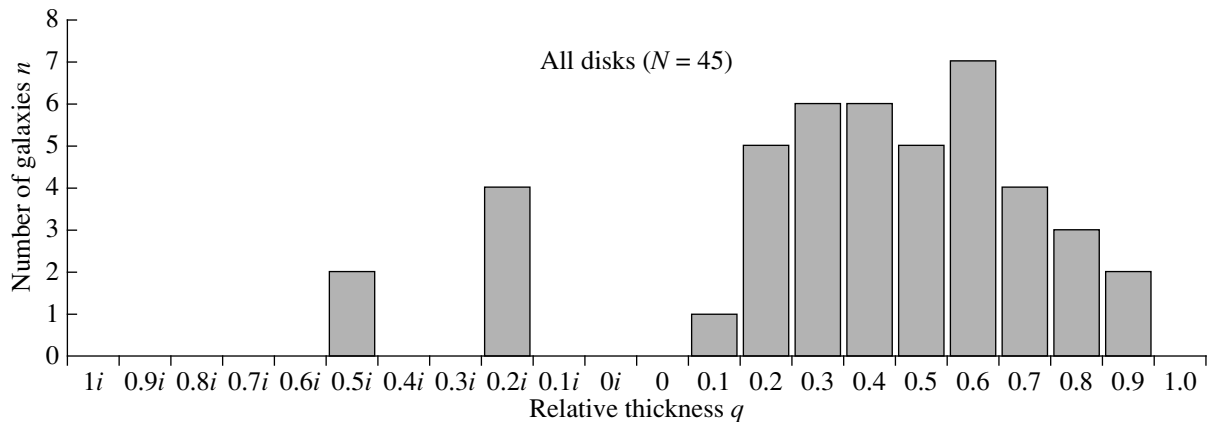


Fig. 3. Distributions of the relative thicknesses q of all the stellar disks analyzed. The “complex” region to the left contains objects that have formally negative arguments of the square root in (3); these are either very thin disks with $q \approx 0$, which ended up in the $0.2i$ bin due to the statistical uncertainty in square of the magnitude q , or disks whose shapes have appreciable inner ellipticity—to those probably belong two discs in the bin $0.5i$.

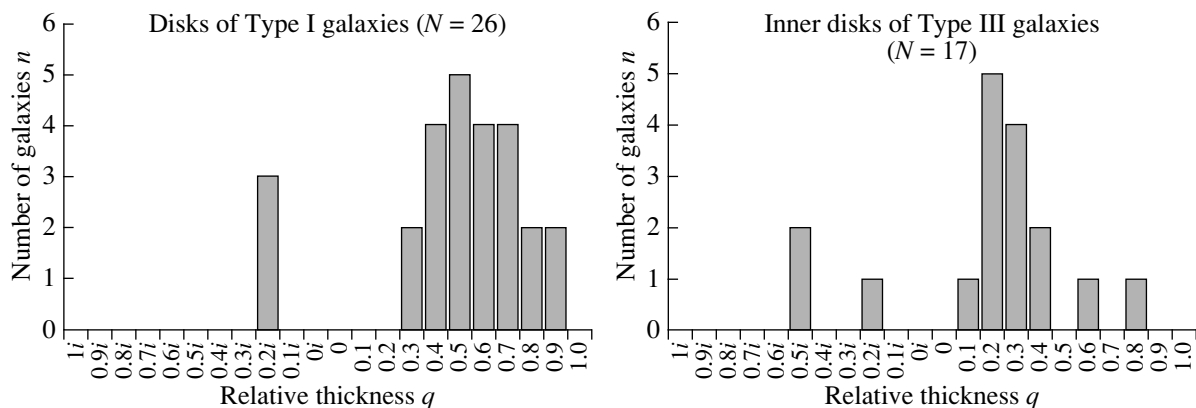


Fig. 4. Comparison of the distributions of the relative disk thicknesses in the Type I galaxies (single-exponential disks) and the inner disks of the Type III galaxies (two-tiered piecewise-exponential disks).

significantly different, with Type I galaxies (single-exponential disks with a single scale throughout) having thicker disks.

It is interesting that, if the galaxies are divided into lenticular and spiral galaxies, or into galaxies with or without bars, the difference in the disk thickness is not so significant. For example, the mean disk thickness for lenticular galaxies without bars is 0.26, while lenticular galaxies with bars have a mean disk thicknesses of 0.46 (Fig. 5). However, both subsamples show a marked scatter of the values. A Kolmogorov–Smirnov test indicates that the probability that the galaxies with and without bars belong to the same parent distribution in terms of their disk thickness is 38%. If we consider the SA0 and SB0 galaxies as one subgroup (S0) and compared them to the spiral galaxies, the statistical difference becomes even lower. The mean relative disk thickness for all the lenticular galaxies is 0.36, and for the spiral galaxies

0.38 (Fig. 6). A Kolmogorov–Smirnov test indicates that the probability that these values are drawn from the same parent distribution is 99.5%.

5. COMPARISON OF RESULTS WITH EARLIER STATISTICS

We compared our results with earlier statistics using the sample of edge-on galaxies compiled by Mosenkov et al. [7], who considered a sample of galaxies from the 2MASS survey satisfying the following criteria.

1. The galaxies are viewed strictly edge-on, $i = 90^\circ$;
2. The ratio of the axes in the summed $J + H + K$ image exceeds 0.2.
3. The radius of the galaxy in the K filter $R_{K_{\text{ron}}} > 30''$.
4. The galaxies are non-interacting.

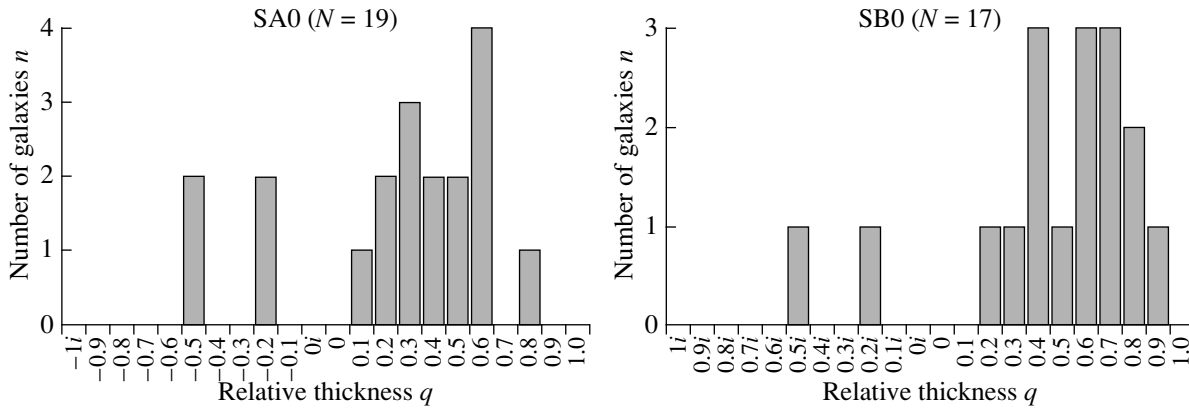


Fig. 5. Comparison of the distributions of the relative disk thicknesses in lenticular galaxies with (SB0) and without (SA0) bars.

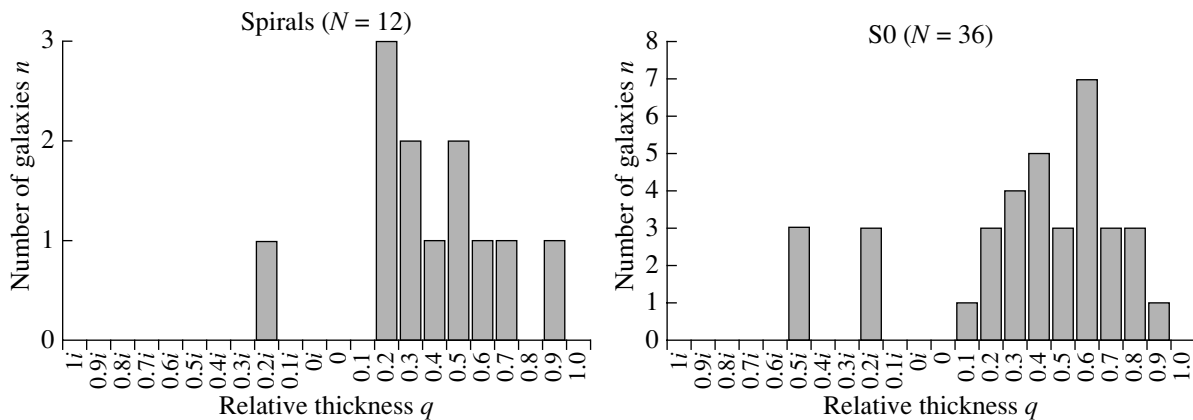


Fig. 6. Comparison of distributions of the relative disk thicknesses in lenticular and spiral (Sa–Sb) galaxies.

5. The concentration index exceeds 2.0.

This yielded a sample of 175 galaxies of all types, whose JHK images were decomposed [7]. The radial component of the brightness profile was approximated using an exponential law with scale h , and the component of the surface brightness profile orthogonal to the equatorial plane using a squared secant law with scale z_0 . The ratio of our parameters a and d and the ratio of the scales h and z_0 are physically different quantities. Nevertheless, it is reasonable to compare the *distributions* of d/a and z_0/h , which are different estimators of the relative thicknesses of the galactic disks. We selected early-type galaxies (S0–Sb) from the sample of [7] for this comparison, for which we calculated $p = z_0/h$ using a table of the disk parameters kindly provided by N.Ya. Sotnikova. We present histograms of p for the resulting subsample of 82 galaxies.

The mean relative thickness for all the subsamples (Fig. 7) is 0.41; the scatter of these values is not

large—83% lie between 0.3 and 0.5. Nevertheless, although the mean disk thicknesses for our sample and the sample [7] are similar, a Kolmogorov–Smirnova test indicates that the probability that our total sample and the subsample from [7] belong to the same parent sample is only 1.7%. The mean disk thickness for the sample from [7] is closest to our subsample of Type I galaxies, but they are also statistically distinguishable. This may be associated with the small size of our sample of Type I galaxies. Breaking down the sample [7] according to morphological type does not lead to appreciable changes in the character of the distribution, as for our own subsamples.

The mean disk thicknesses of lenticular and edge-on spiral galaxies are not significantly different: 0.40 and 0.42 (Fig. 8). This is also in qualitative agreement with our results. However, the scatter of values for these galaxies is more substantial: only 76% of lenticular galaxies have p values from 0.3 to 0.5, while the distribution of thicknesses is more compact for the spiral galaxies: 89% have p values in the

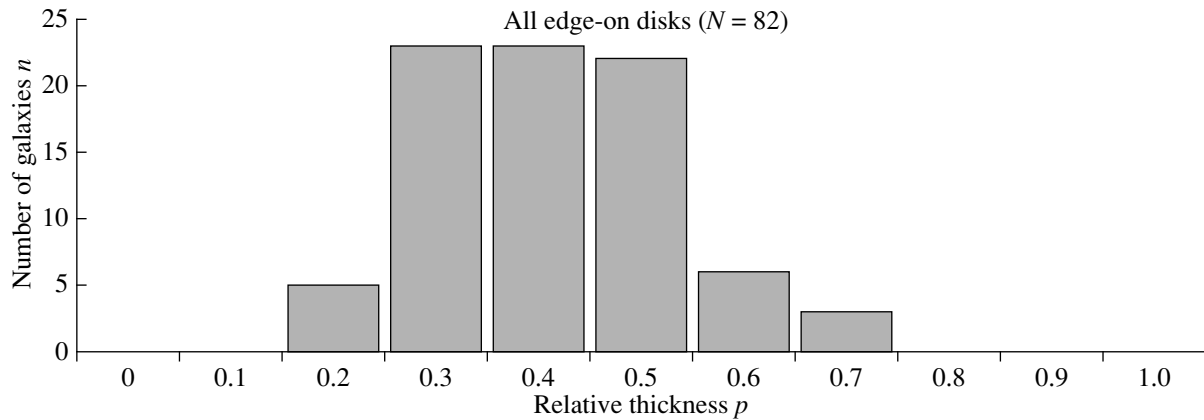


Fig. 7. Distribution of relative disk thickness in edge-on galaxies from [7] (morphological type S0–Sb, NIR J band).

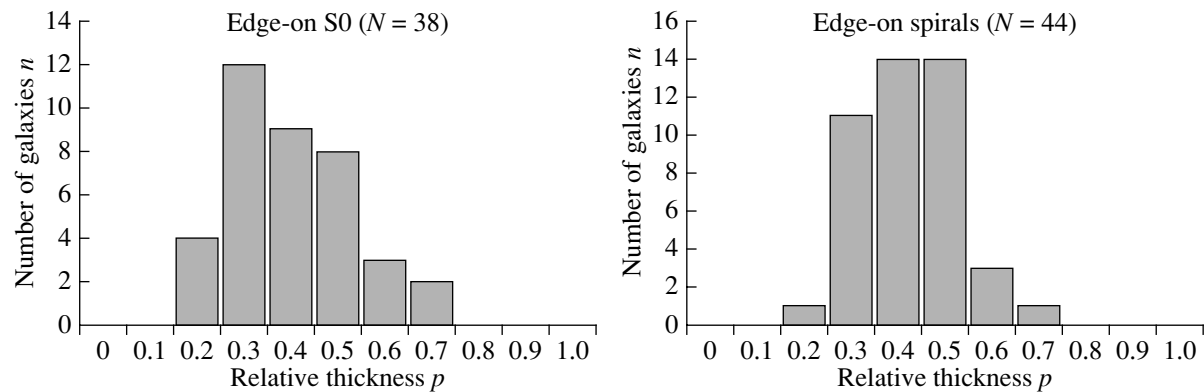


Fig. 8. Comparison of the distributions of relative disk thickness for edge-on lenticular and spiral (Sa–Sb) galaxies according to the decomposition of their J -band images from [7].

range [0.3, 0.5]. A Kolmogorov–Smirnov test indicates an absence of significant differences between the disk thicknesses for galaxies of various morphological types: the probability that both subsamples belong to the same distribution is 76%. Thus, our sample and the sample from [7] are similar in the sense that, among early-type disk galaxies, there is no significant difference in the disk thicknesses of lenticular and spiral galaxies.

6. CONCLUSIONS AND DISCUSSION

We have proposed a new method for deriving the relative thickness of a galactic disk from the two-dimensional distribution of its surface brightness in the plane of the sky. We have applied this method to 45 early-type (S0–Sb) galaxies with exponential (Type I according to [8, 9]) or piecewise-exponential (with a flatter outer profile, Type III according to [8, 9]). The resulting statistics for the relative disk thicknesses of early-type galaxies reveals a number

of interesting features. On average, the disks of lenticular and early-type spiral galaxies have similar thicknesses. The presence of a bar leads to only a marginal thickening of the disks. However, there is a significant difference between the thicknesses of disks with single-exponential brightness profiles and the inner portions of disks with Type III profiles (i.e., with outer exponential disks having larger scales). The disks are significantly thicker in the former than in the latter case.

How should we interpret these similarities and differences in the framework of modern ideas about the origin and evolution of the stellar disks of galaxies? The origin of the exponential brightness (density) profiles of the disks remains a mystery. In the recent observational analytical study [16], it is noted that a single exponential profile can extend over the entire galaxy, including areas with very different star-formation modes and time scales. This seemingly contradicts the idea that an exponential density profile develops in the course of the disk's evolution, and

provides evidence that an initially exponential density profile with a fixed scale is a necessary initial condition for the evolution of a stellar disk. However, if star formation proceeds in different modes and on different time scales in different regions of a galaxy, why is the initial density profile not “smeared out” over a time scale of a few billion years?

A completely opposite paradigm seems to be more physical. This picture was semi-qualitatively, semi-analytically developed by Lin and Pringle [17] in the 1980s, and was later elaborated in more detail and confirmed by numerical models by Slyz et al. [18]. These studies considered a violent radial redistribution of matter occurring in parallel with star formation. If a gaseous galactic disk is strongly viscous and the viscosity time scale is comparable to the star-formation time scale, an exponential stellar disk is naturally constructed. This model is not very popular, first and foremost because the viscosity must be very strong. However, at large redshifts $z > 2$, when relatively cool gas contributed a dominant share of the baryonic matter in galaxies and clumps with very different sizes formed in the disks due to various instabilities and “floated” in the more diffuse gas, the viscosity could be considerably higher than at the current epoch.

Investigating the stellar populations at the centers of galaxies with single-exponential disk-brightness profiles (Type I), we have already received indirect confirmation that radial inflow of the gas into the centers of galaxies was especially intense in Type I disks. We found chemically distinct nuclei with especially large metallicity differences between the nucleus and bulge in the centers of a sample of Type I galaxies [19]. If Type I galaxies have experienced the most violent radial redistribution of gas during their evolution, it is possible that the same processes that removed the angular momentum of the gas (transient bars of a tidal nature, for example) also dynamically heated the stellar disk. This could explain the presence of thicker stellar disks in such galaxies.

The origin of Type III disks is currently explained by minor mergers, according to the dynamical numerical models of Younger et al. [20]. These models show that the outer exponential segment of the disk brightness profile (which has the larger exponential scale) builds up in the process of minor mergers with old disk stars of the primary (“parent”) galaxy, which are undergoing a violent outward migration due to the action of a satellite that has impacted the disk. If the absorbed satellite also contained gas, it flows down into the central region of the galaxy and, after the resulting burst of star formation, adds a young, cool stellar population to the inner disk. This scenario can qualitatively explain the small thicknesses of the inner disks of Type III galaxies and the fact that, when we

are able to investigate them, the corresponding outer disks have larger thickness than the inner disks.

ACKNOWLEDGMENTS

We thank N.Ya. Sotnikova for providing the results of the image decomposition for edge-on galaxies from [7] in tabular form. We have used the Lyon–Meudon extragalactic database (LEDA), which is supported by the LEDA team in the Lyon Observatory CRAL (France), and the NASA/IPAC Extragalactic Database (NED), which is operated by the Jet Propulsion Laboratory, California Institute of Technology, under contract with the National Aeronautics and Space Administration. We have made use of the public archives of the SDSS-III survey (<http://www.sdss3.org>), which is supported by Alfred P. Sloan Foundation, the participant institutes of the SDSS collaboration, National Science Foundation, and the United States Department of Energy.

REFERENCES

1. T. Miwa and M. Noguchi, *Astrophys. J.* **499**, 149 (1998).
2. I. R. Walker, J. Ch. Mihos, and L. Hernquist, *Astrophys. J.* **460**, 121 (1996).
3. V. Reshetnikov and F. Combes, *Astron. Astrophys.* **324**, 80 (1997).
4. N. D. Padilla and M. A. Strauss, *Mon. Not. R. Astron. Soc.* **388**, 1321 (2008).
5. S. Rodríguez and N. D. Padilla, *Mon. Not. R. Astron. Soc.* **434**, 2153 (2013).
6. R. de Grijs and P. C. van der Kruit, *Astron. Astrophys. Suppl. Ser.* **117**, 19 (1996).
7. A. V. Mosenkov, N. Ya. Sotnikova, and V. P. Reshetnikov, *Mon. Not. R. Astron. Soc.* **401**, 559 (2010).
8. P. Erwin, V. Pohlen, and J. E. Beckman, *Astron. J.* **135**, 20 (2008).
9. L. Gutiérrez, P. Erwin, R. Aladro, and J. E. Beckman, *Astron. J.* **142**, 145 (2011).
10. K. C. Freeman, *Astrophys. J.* **160**, 767 (1970).
11. H. Aihara, C. Allende Prieto, D. An, S. F. Anderson, E. Aubourg, E. Balbinot, T. C. Beers, A. A. Berlind, S. J. Bickerton, D. Bizyaev, M. R. Blanton, J. J. Bochanski, A. S. Bolton, J. Bovy, W. N. Brandt, J. Brinkmann, P. J. Brown, J. R. Brownstein, N. G. Busca, H. Campbell, M. A. Carr, Y. Chen, C. Chiappini, J. Comparat, N. Connolly, M. Cortes, R. A. C. Croft, A. J. Cuesta, L. N. da Costa, J. R. A. Davenport, K. Dawson, S. Dhital, A. Ealet, G. L. Ebelke, E. M. Edmondson, D. J. Eisenstein, S. Escoffier, M. Esposito, M. L. Evans, X. Fan, B. Femenía Castellá, A. Font-Ribera, P. M. Frinchaboy, J. Ge, B. A. Gillespie, G. Gilmore, J. I. González Hernández, J. R. Gott, A. Gould, E. K. Grebel, J. E. Gunn, J.-Ch. Hamilton, P. Harding, D. W. Harris, S. L. Hawley, F. R. Hearty,

- S. Ho, D. W. Hogg, J. A. Holtzman, K. Honscheid, N. Inada, I. I. Ivans, L. Jiang, J. A. Johnson, C. Jordan, W. P. Jordan, E. A. Kazin, D. Kirkby, M. A. Klaene, G. R. Knapp, J.-P. Kneib, C. S. Kochanek, L. Koesterke, J. A. Kollmeier, R. G. Kron, H. Lampeitl, D. Lang, J.-M. Le Goff, Y. S. Lee, Y.-T. Lin, D. C. Long, C. P. Loomis, S. Lucatello, B. Lundgren, R. H. Lupton, Zh. Ma, N. MacDonald, S. Mahadevan, M. A. G. Maia, M. Makler, E. Malanushenko, V. Malanushenko, R. Mandelbaum, C. Maraston, D. Margala, K. L. Masters, C. K. McBride, P. M. McGehee, I. D. McGreer, B. Ménard, J. Miralda-Escudé, H. L. Morrison, F. Mullally, D. Muna, J. A. Munn, H. Murayama, A. D. Myers, T. Naugle, A. Fausti Neto, D. C. Nguyen, R. C. Nichol, R. W. O'Connell, R. L. C. Ogando, M. D. Olmstead, D. J. Oravetz, N. Padmanabhan, N. Palanque-Delabrouille, K. Pan, P. Pandey, I. Paris, W. J. Percival, P. Petitjean, R. Pfaffenberger, J. Pforr, S. Phleps, Ch. Pichon, M. M. Pieri, F. Prada, A. M. Price-Whelan, M. J. Raddick, B. H. F. Ramos, C. Reylé, J. Rich, G. T. Richards, H.-W. Rix, A. C. Robin, H. J. Rocha-Pinto, C. M. Rockosi, N. A. Roe, E. Rollinde, A. J. Ross, N. P. Ross, B. M. Rossetto, A. G. Sánchez, C. Sayres, D. J. Schlegel, K. J. Schlesinger, S. J. Schmidt, D. P. Schneider, E. Sheldon, Y. Shu, J. Simmerer, A. E. Simmons, T. Sivarani, S. A. Snedden, J. S. Sobeck, M. Steinmetz, M. A. Strauss, A. S. Szalay, M. Tanaka, A. R. Thakar, D. Thomas, J. L. Tinker, B. M. Tofflemire, R. Tojeiro, Ch. A. Tremonti, J. Vandenberg, M. Vargas Magana, L. Verde, N. P. Vogt, D. A. Wake, J. Wang, B. A. Weaver, D. H. Weinberg, M. White, S. D. M. White, B. Yanny, N. Yasuda, Ch. Yeche, and I. Zehavi, *Astrophys. J. Suppl. Ser.* **193**, 29 (2011).
12. V. L. Afanasiev and A. V. Moiseev, *Astron. Lett.* **31**, 194 (2005).
 13. M. A. Il'ina and O. K. Sil'chenko, *Astron. Lett.* **37**, 589 (2011).
 14. A. V. Zasov, O. K. Sil'chenko, I. Yu. Katkov, and S. N. Dodonov, *Astron. Lett.* **39**, 17 (2013).
 15. O. K. Sil'chenko, I. V. Chilingarian, N. Ya. Sotnikova, and V. L. Afanasiev, *Mon. Not. R. Astron. Soc.* **414**, 3645 (2011).
 16. D. A. Hunter, B. C. Elmegreen, V. C. Rubin, A. Ashburn, T. Wright, G. I. G. Józsa, and Ch. Struve, *Astron. J.* **146**, 92 (2013).
 17. D. N. C. Lin and J. E. Pringle, *Astrophys. J. Lett.* **320**, L87 (1987).
 18. A. D. Slyz, J. E. Devriendt, J. Silk, and A. Burkert, *Mon. Not. R. Astron. Soc.* **333**, 894 (2002).
 19. O. K. Sil'chenko and I. V. Chilingarian, *Astron. Lett.* **37**, 1 (2011).
 20. J. D. Younger, T. J. Cox, A. C. Seth, and L. Hernquist, *Astrophys. J.* **670**, 269 (2007).

Translated by L. Yungel'son